Available online at www.sciencedirect.com

SCIENCE DIRECT

Virology 342 (2005) 297 – 310

VIROLOGY

www.elsevier.com/locate/yviro

# Herpes simplex virus 2 modulates apoptosis and stimulates NF-κB nuclear translocation during infection in human epithelial HEp-2 cells

Jamie C. Yedowitz, John A. Blaho*

*Department of Microbiology, Mount Sinai School of Medicine, One Gustave L. Levy Place, New York, NY 10029-6574, USA*

Received 6 June 2005; returned to author for revision 11 July 2005; accepted 20 July 2005
Available online 15 September 2005

**Abstract**

Virus-mediated apoptosis is well documented in various systems, including herpes simplex virus 1 (HSV-1). HSV-2 is closely related to HSV-1 but its apoptotic potential during infection has not been extensively scrutinized. We report that (i) HEp-2 cells infected with HSV-2(G) triggered apoptosis, assessed by apoptotic cellular morphologies, oligosomal DNA laddering, chromatin condensation, and death factor processing when a translational inhibitor (CHX) was added at 3 hpi. Thus, HSV-2 induced apoptosis but was unable to prevent the process from killing cells. (ii) Results from a time course of CHX addition experiment indicated that infected cell protein produced between 3 and 5 hpi, termed the apoptosis prevention window, are required for blocking virus-induced apoptosis. This corresponds to the same prevention time frame as reported for HSV-1. (iii) Importantly, CHX addition prior to 3 hpi led to less apoptosis than that at 3 hpi. This suggests that proteins produced immediately upon infection are needed for efficient apoptosis induction by HSV-2. This finding is different from that observed previously with HSV-1. (iv) Infected cell factors produced during the HSV-2(G) prevention window inhibited apoptosis induced by external TNFα plus cycloheximide treatment. (v) NF-κB translocated to nuclei and its presence in nuclei correlated with apoptosis prevention during HSV-2(G) infection. (vi) Finally, clinical HSV-2 isolates induced and prevented apoptosis in HEp-2 cells in a manner similar to that of laboratory strains. Thus, while laboratory and clinical HSV-2 strains are capable of modulating apoptosis in human HEp-2 cells, the mechanism of HSV-2 induction of apoptosis differs from that of HSV-1.


*Keywords:* HSV-2; Apoptosis; NF-κB; Clinical virus isolates

## Introduction

Apoptosis is the purposeful process of cell suicide characterized by distinct features including condensation of the cell, maintenance of organelle integrity, and plasma membrane blebbing (reviewed in Kerr et al., 1972; Sanfilippo and Blaho, 2003). Apoptosis is also an important cellular response to virus infection, and many viruses, especially the large DNA viruses, have evolved mechanisms to block the process (Koyama et al., 2000). Recently, a large body of information has been generated which describes apoptosis during HSV-1 infection (reviewed in Goodkin et al., 2004). Briefly, HSV-1 triggers apoptosis and then later infected cell proteins block the process from killing the cell, thus modulating the cell death process (reviewed in Aubert and Blaho, 2001). The survival factors produced in this "prevention window" not only block apoptosis triggered by the virus but also that stimulated by numerous external or environmental pro-apoptotic treatments. The cellular transcription factor NF-κB becomes activated during HSV-1 infection (Amici et al., 2001; Patel et al., 1998). While its presence in nuclei correlates with apoptosis prevention (Goodkin et al., 2003; Gregory et al., 2004; Medici et al., 2003), alternative roles for NF-κB during HSV-1 infection have also been proposed (Taddeo et al., 2002). Conversely, the status of apoptosis during HSV-2 infection is much less clear.

When Koyama et al. looked at apoptosis during HSV-2 infection, they observed a small but significant level of apoptosis in HSV-2-infected HEp-2 cells, in contrast to HSV-1 (Koyama et al., 1998). Apoptotic features were also

* Corresponding author. Fax: +1 212 534 1684.
*E-mail address:* john.blaho@mssm.edu (J.A. Blaho).

0042-6822/$ - see front matter © 2005 Elsevier Inc. All rights reserved.
doi:10.1016/j.virol.2005.07.036

observed during HSV-2 infection of dorsal root ganglia, lumbar spinal cord (Ozaki et al., 1997), pituitary gland, peritoneal macrophages (Fleck et al., 1999), monocytoid (Mastino et al., 1997), and dendritic cells (Jones et al., 2003). Together, these observations seem to imply that infection with wild-type HSV-2 leads to apoptotic cell death. A series of experiments by Jerome and Corey showed that HSV-2 was unable to block antigen-specific CD4+ cytotoxic T-lymphocyte (Jerome et al., 1998)-, UV-, and anti-Fas antibody (Jerome et al., 1999)-induced apoptosis, suggesting that differences exist between HSV-1 and HSV-2 in their ability to inhibit apoptosis. Consistent with these observations is the finding that HSV-2, but not HSV-1, blocks the surface expression and activity of Fas ligand (Sieg et al., 1996). However, others have concluded that HSV-2 can indeed prevent apoptosis in a manner similar to HSV-1 and the viral $U_S3$ protein kinase (Asano et al., 1999; Hata et al., 1999) and ribonucleotide reductase (Langelier et al., 2002; Perkins et al., 2003) participate in the blocking. One explanation for such apparent inconsistencies is that the HSV-2 anti-apoptotic effect may result from laboratory adaptation since primary clinical HSV-2 isolates were reported to be unable to block apoptosis (Jerome et al., 2001). These issues described above indicate the status of apoptosis during HSV-2 infection is currently unresolved.

The goal of this study is to determine whether HSV-2 strains have the ability to modulate apoptosis during infection. We show that both clinical and laboratory HSV-2 strains induced and subsequently blocked apoptosis in infected HEp-2 cells. HSV-2-infected cell proteins synthesized between 3 and 5 hpi were required for blocking apoptosis triggered either by virus infection or environmental TNFα plus cycloheximide treatment. NF-κB translocated to the nuclei of HSV-2-infected cells and this correlated with apoptosis prevention. In contrast to HSV-1, optimal HSV-2-induced apoptosis appeared to required infected cell proteins produced immediately upon infection. Together, these results imply that the prevention of apoptosis by HSV-2 and HSV-1 is similar, but the mechanism or efficiency of induction by the two viruses may differ.

## Results

### *Induction and prevention of apoptosis in HSV-2(G)-infected HEp-2 cells*

HEp-2 cells infected with wild-type HSV-1 in the presence of CHX die of apoptosis (Aubert and Blaho, 1999; Koyama and Adachi, 1997). While IE gene expression triggers apoptosis in HSV-1-infected cells (Sanfilippo et al., 2004), infected cell proteins produced between 3 and 6 hpi in an apoptosis "prevention window" prevent the process from killing the infected cells (Aubert et al., 1999). In this manner, HSV-1 modulates the programmed cell death process during its productive replication cycle (Aubert and Blaho, 2001; Goodkin et al., 2004). The goal of this study was to determine whether HSV-2-infected HEp-2 cells manipulate apoptosis in a similar manner to that described for HSV-1-infected cells.

To investigate apoptosis during HSV-2 infection, we performed three series of experiments. In the first set, HEp-2 cells were mock-infected, infected with HSV-1(F) or HSV-2(G), and either subjected to CHX additions at 3 and 6 hpi or not treated at all. For control purposes, mock-infected cells were maintained in the presence and absence of CHX to reveal any background levels of apoptosis due to CHX. In addition, TNFα plus CHX (TNFα/CHX) were added to cells at 0 hpi as a positive control. At 17 hpi, live cells were stained with Hoechst DNA dye and subsequently visualized by microscopy to observe nuclear and cellular morphologies as described in Materials and methods. Intense, compact nuclear blue fluorescent staining corresponds to cells that have condensed chromatin, a characteristic of apoptosis (Aubert and Blaho, 1999). Apoptotic cells also display various morphological characteristics, such as membrane blebbing, cell shrinkage, nuclear condensation, and chromatin margination which are readily visualized by standard light microscopy (Kerr et al., 1972; Sanfilippo and Blaho, 2003). The results (Fig. 1A) were as follows.

As expected (Aubert and Blaho, 1999), little to no apoptotic features were observed in mock-infected cells in the absence and presence of CHX (2% and 7% condensed chromatin, respectively) (Fig. 1A, panels 1 and 3). Almost complete condensation of chromatin (94%) and cell shrinkage/membrane blebbing occurred in the control TNFα/CHX-treated cells (panels 5 and 6). Cytopathic effect was observed with HSV-1(F) and HSV-2(G) in the absence of CHX (compare panel 2 with panels 8 and 14). The addition of CHX at 3 hpi to HSV-1(F)- and HSV-2(G)-infected cells resulted in dramatic increases in condensed chromatin (69% and 67%, respectively) with many cells showing apoptotic morphologies (panels 9, 10 and 15, 16). Thus, when infected cell protein synthesis is prevented at 3 hpi (by addition of CHX), the infected cells readily die. Comparison of the HSV-1- and HSV-2-infected cells without and with the addition of CHX at 3 hpi demonstrated a dramatic increase in cells displaying condensed chromatin (from 6% to 69% for HSV-1(F) and from 5% to 67% for HSV-2(G)). This represents an approximately 12-fold difference for HSV-2 and a 10-fold change for HSV-1, demonstrating that the effects are similar for the two viruses. The addition of CHX at 6 hpi resulted in a significant decrease in the number of cells undergoing apoptosis (an approximately 30–40% drop) compared to CHX addition at 3 hpi (compare 12, 18 with 10, 16). These findings imply that HSV-2(G) may be capable of inducing apoptosis in HEp-2 and that proteins necessary for apoptosis prevention may be synthesized prior to 6 hpi.

In the next set of experiments, we further investigated these results from a biochemical standpoint. The cells shown

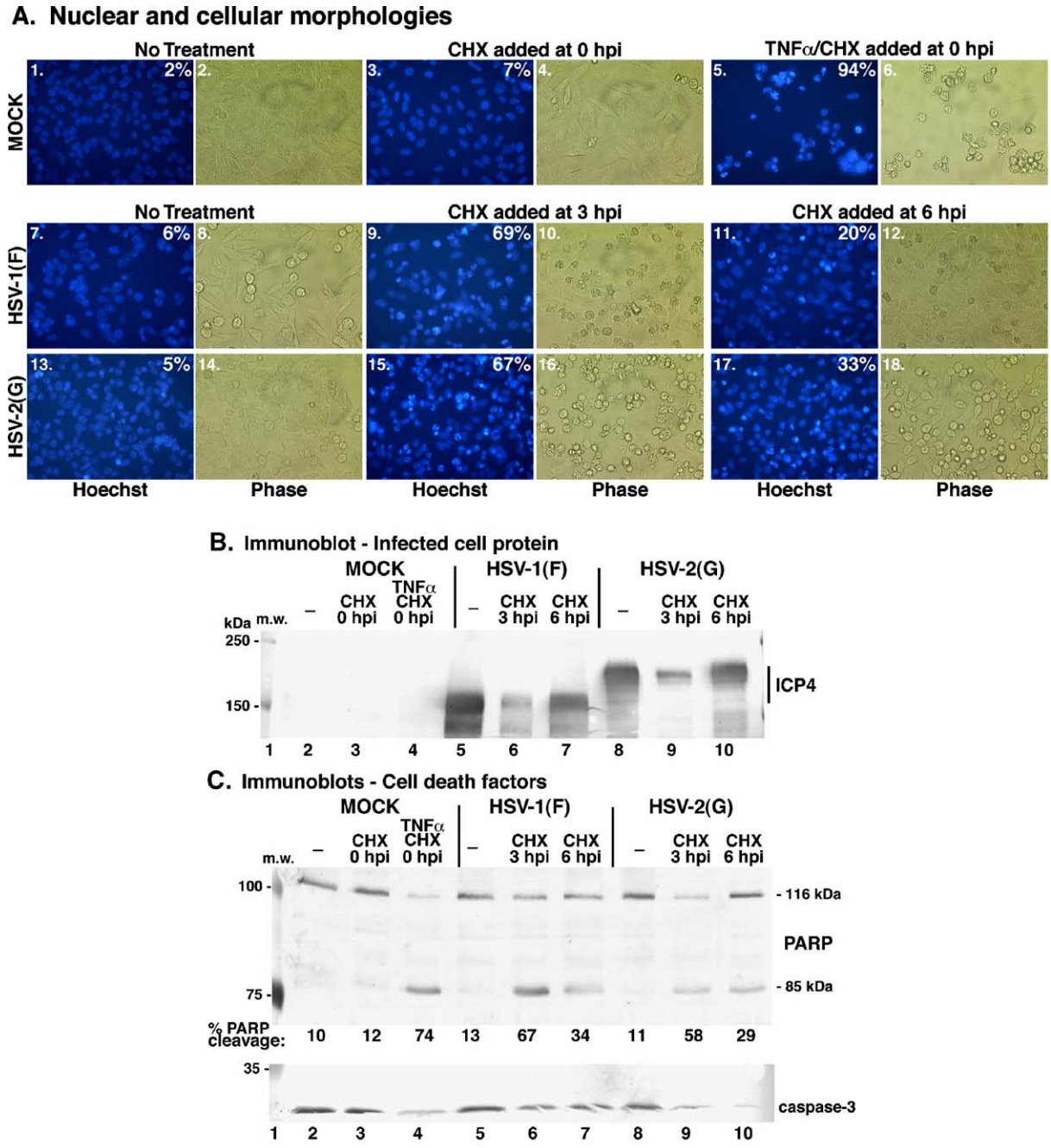


Fig. 1. Infected cell morphologies (A) and immunoblots of infected cell proteins (B) and death factors (C). Mock-, HSV-1(F)-, and HSV-2(G)-infected cells (MOI of 10 PFU/cell) were either CHX treated, CHX/TNFα treated, or not treated at all (−) at the corresponding times indicated. Phase-contrast and Hoechst (H33258)-stained fluorescence images were obtained at 17 hpi (A). White numbers in the right corners correspond to the number of apoptotic cells (magnification ×40). Whole cell extracts were prepared at 18 hpi, separated in a denaturing gel, transferred to nitrocellulose, and probed with anti-ICP4, anti-α-tubulin (A), anti-PARP, and anti-caspase-3 (B) antibodies. Percentage of PARP cleavage was determined using NIH image. Locations of molecular mass (kDa) markers are indicated in the margins.

in Fig. 1A were harvested at 18 hpi, whole cell extracts were prepared, separated in a denaturing gel, transferred to nitrocellulose, and probed using anti-ICP4, anti-PARP, and anti-caspase-3 antibodies as described in Materials and methods. Blots were also probed with an anti-α-tubulin antibody as a loading control to ensure that each lane received an equal amount of protein (data not shown). ICP4 was used as a marker for infection since the slight mobility shift of ICP4 allows us to unambiguously differentiate between HSV-1- and HSV-2-infected cells (Blaho and Roizman, 1991; Blaho et al., 1994). During apoptosis, the inactive form of caspase-3 (procaspase-3) becomes cleaved and PARP is processed from its full-length 116-kDa form to a cleaved product of 85 kDa (Sanfilippo and Blaho, 2003); in

our system, PARP cleavage (quantitated as described in Materials and methods) and the loss of anti-caspase-3 antibody reactivity are indicative of apoptotic processing.

While ICP4 from HSV-1 and HSV-2 was synthesized to abundant levels in infected cells in the absence of CHX (Fig. 1B, lanes 5 and 8), levels of ICP4 significantly decreased when CHX was added at 3 hpi (lanes 6 and 9). ICP4 levels approached that of non-treated cells when CHX was added at 6 hpi (compare lanes 5, 8 with lanes 7, 10). Mock-infected cells in the presence and absence of CHX revealed background levels (10% and 12%) of PARP cleavage (Fig. 1C, lanes 2 and 3) and no caspase-3 activation (lanes 2 and 3). The most PARP cleavage (74%) was found with control TNFα/CHX added at 0 hpi (lane 4). The amount of PARP and caspase-3 cleavage in HSV-1(F)- and HSV-2(G)-infected cells in the absence of CHX was comparable to mock-infected cells (compare lanes 5 and 8 with lane 2). The addition of CHX at 3 hpi to HSV-1- and HSV-2-infected cells resulted in an approximately five-fold increase of PARP cleavage compared to non-treated cells (compare lane 5 with lane 6 and lane 8 with lane 9). When CHX was added at 6 hpi, the percentage of PARP cleavage was reduced from 67% to 34% in HSV-1-infected cells (lanes 6 and 7) and 58% to 29% in HSV-2-infected cells (lanes 8 and 10), representing an approximately 2-fold difference for each virus. Caspase-3 activation appeared to mirror these observations as the disappearance of caspase-3 increased significantly when CHX was added at 3 hpi (lanes 6 and 9).

In the final set of experiments, HEp-2 cells mock infected or infected with HSV-1(F) or HSV-2(G) were treated with CHX or TNFα/CHX as in Fig. 1, then harvested at 22 hpi, and a DNA fragmentation assay (Fig. 2) was performed as described in Materials and methods. Mock-infected cells with no treatment resulted in a very minimal amount of fragmentation (Fig. 2, lane 1) while cells treated with TNFα/CHX at 0 hpi resulted in the most fragmentation, as evidenced by a smear (lane 3). The progression from a defined oligonucleotide ladder at early times of apoptosis followed by a definitive smear later is standard for HEp-2 cells (Aubert and Blaho, 1999; Nguyen et al., 2005). Non-treated HSV-1(F)- and HSV-2(G)-infected cells displayed fragmentation similar to that of control mock-infected cells (compare lanes 4 and 8 with lanes 1 and 2). The amount of DNA fragmentation increased significantly in HSV-1(F)- and HSV-2(G)-infected cells treated with CHX at 3 hpi, comparable to that with TNFα/CHX (compare lanes 5 and 7 with lane 3), while CHX addition at 6 hpi was much reduced (lanes 6 and 9). It should be noted that since these were low molecular weight DNA preparations, increased total DNA, as observed in lanes 3, 5, and 7, corresponds to DNA liberated during apoptosis (Aubert and Blaho, 1999; Nguyen et al., 2005). Based on all of these findings, we can conclude that HSV-2(G) has the ability to first induce and then block apoptosis. When CHX was added at 3 hpi, apoptosis was triggered in the infected cells

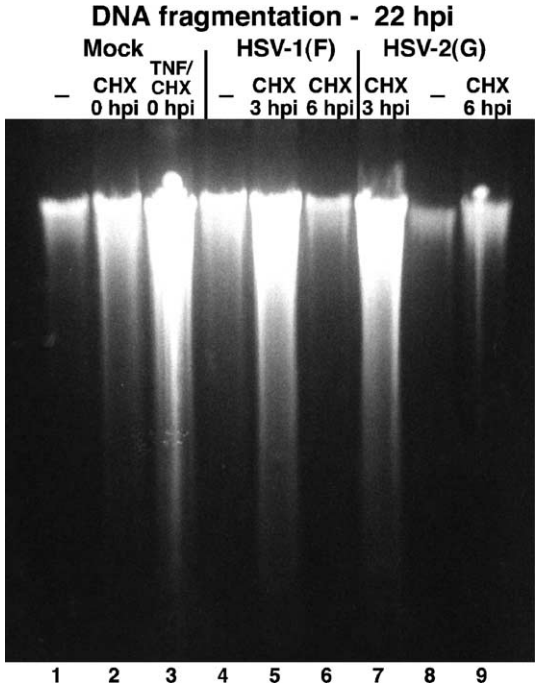


Fig. 2. Nucleosomal laddering of chromosomal DNA was extracted from HSV-1(F)-, HSV-2(G)-, and mock-infected HEp-2 cells (MOI of 10 PFU/cell). Cells were either treated with CHX (10 μg/μl), TNFα/CHX (10 μg/μl), or not at all (−) at the times indicated. DNA was extracted at 22 hpi, separated in a 1.5% agarose gel containing ethidium bromide (0.1% μg/ml), and visualized under UV illumination.

but they died because they were unable to synthesize sufficient levels of the necessary proteins required to block the death process, yielding morphological, biochemical, and genetic apoptotic features.

### *Determination of the HSV-2(G) apoptosis prevention window time frame*

As previously described (Aubert et al., 1999) and observed above, wild-type HSV-1 induces but then blocks apoptosis and this prevention requires de novo synthesis of infected cell proteins between 3 and 5 hpi (Moy and Blaho, unpublished results). Since HSV-2 has a faster rate of infection then HSV-1 in cultured cells (Blaho and Roizman, 1991; Blaho et al., 1994), we needed to examine the kinetics of apoptosis prevention by HSV-2(G). HEp-2 cells were mock infected or infected with HSV-2(G) and CHX was either not added or added at various time points during infection (0–8 hpi) to block de novo protein synthesis. Whole cell extracts were prepared at 21 hpi, separated on a denaturing gel, transferred to nitrocellulose, and probed using anti-ICP4, anti-α-tubulin, anti-PARP, and anti-caspase-3 antibodies as described in Materials and methods. We probed for α-tubulin as a loading control to ensure that every lane received equal amounts of protein. The results (Fig. 3) were as follows.

The level of ICP4 detected in HSV-2(G)-infected cells in the absence of CHX was comparable to that observed when

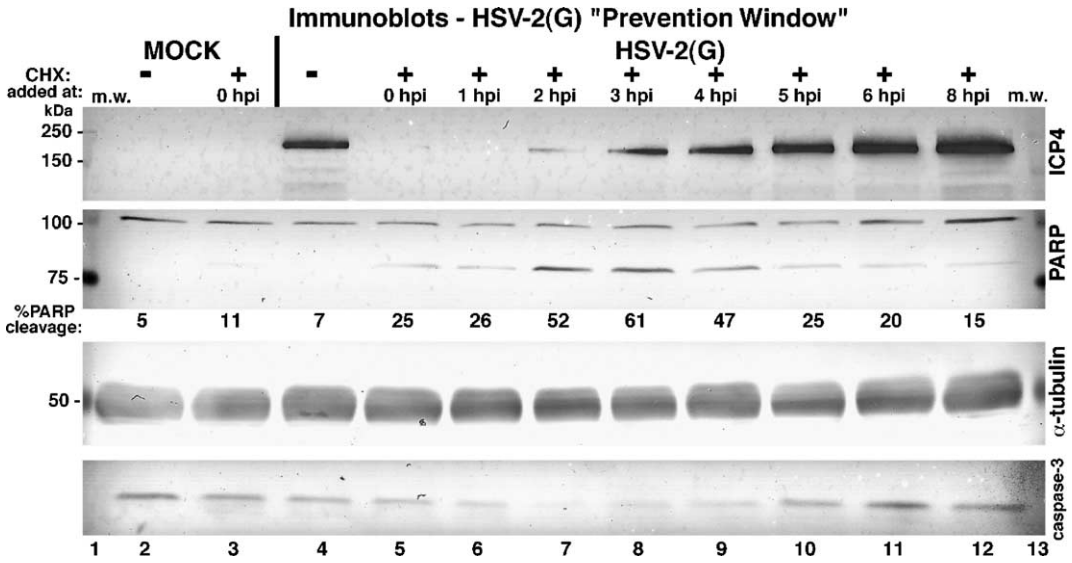


Fig. 3. Identification of the HSV-2(G) apoptosis prevention window. Whole cell extracts were prepared at 22 hpi from mock-infected cells or cells infected with HSV-2(G) (MOI of 10 PFU/cell), separated in a denaturing gel, transferred to nitrocellulose, and probed with anti-ICP4, anti-α-tubulin, anti-PARP, and anti-caspase-3 antibodies. Infected cells were treated (+) with CHX (10 μg/μl) at the times indicated or not treated at all (−). Mock-infected cells treated with CHX (10 μg/μl) were used as a control. PARP cleavage was quantified using NIH Image. Locations of molecular mass (kDa) markers are indicated in the left margin.

CHX was added at 6 and 8 hpi (Fig. 3, compare lane 4 with lanes 11 and 12). In contrast, the addition of CHX at 0–3 hpi greatly diminished the amounts of ICP4, indicating CHX succeeded in blocking newly synthesized protein. Mock-infected cells, as well as the mock-infected cells with CHX added at 0 hpi, showed low background levels (5% and 11%, respectively) of PARP cleavage (lanes 2 and 3). Cells infected with HSV-2(G) without treatment showed PARP cleavage levels (7%) similar to that of mock-infected (5%) cells (compare lane 4 and lane 2), reiterating that HSV-2(G), in the absence of CHX, does not show features of apoptosis. In contrast, the amount of caspase-3 in the HSV-2(G)-infected cells was slightly less than that of mock (compare lane 4 with lane 2). A similar partial loss of caspase-3 was observed during wild-type HSV-1 infection (Aubert et al., 1999) and implies the induction of "abortive apoptosis" during infection with these viruses (Goodkin et al., 2004).

Maximum PARP cleavage (52% and 61%) was observed during HSV-2(G) infection when CHX was added at 2 and 3 hpi (lanes 6 and 7). While the levels of PARP cleavage observed with the 0- and 1-hpi CHX additions (25% and 26%, respectively) were significantly greater than the control mock (5%) and untreated infected (7%) cells (compare lanes 5, 6 with lanes 2, 4), they were not maximum. This finding was surprising since we (Aubert and Blaho, 1999; Aubert et al., 1999) and others (Koyama and Adachi, 1997) have repeatedly observed that CHX at the time of HSV-1 infection (0 hpi) results in maximum apoptosis. Cleavage of caspase-3 mirrored the PARP processing results, inasmuch as maximum caspase-3 loss was observed when CHX was added at 2 and 3 hpi (lanes 7 and 8). We have repeated this time course of CHX addition experiment five separate times and observed the exact same phenomena (data not shown). That maximum apoptosis with HSV-2(G) occurs when CHX is added at 2 or 3 hpi and suggests a difference in apoptosis modulation between these two viruses.

The cells used above were also visualized at 21 hpi by phase-contrast microscopy prior to extraction (data not shown). Mock-infected cells with no treatment displayed no characteristics of apoptosis, while TNFα/CHX treatment resulted in almost 100% of the cells displaying characteristic apoptotic morphologies. HSV-2(G)-infected cells that received no CHX treatment displayed cytopathic effect and did not appear to be apoptotic. During HSV-2(G) infection, the percentage of cells that appeared apoptotic increased as CHX was added at each sequential hour until 6 hpi, thus corroborating our biochemical data above. Based on these results, we conclude the HSV-1(G) apoptosis prevention window is between 3 and 5 hpi. This time frame is the same as that observed for HSV-1 (Aubert and Blaho, 2001; Aubert et al., 1999).

### *HSV-2(G)-infected cells fail to block TNFα plus CHX apoptotic stimulus when applied at 3 hpi*

The previous studies above focused on the ability of HSV-2 to prevent apoptosis that was triggered by infection with the virus itself. However, apoptosis can be caused by a variety of internal and external triggers (reviewed in Sanfilippo and Blaho, 2003) and HSV-1 has been shown to prevent cell death induced by many of these agents (Galvan and Roizman, 1998; Goodkin et al., 2003; Jerome et al., 1998; Koyama and Miwa, 1997). We were particularly interested in determining what effect the addition of TNFα plus CHX would have on HSV-2(G)-infected HEp-2 cells since we previously reported that infected cell proteins

produced between 3 and 6 hpi during HSV-1 infection block apoptosis induced by these agents (Goodkin et al., 2003). HEp-2 cells were mock, HSV-1(F), or HSV-2(G) infected (MOI = 10 PFU/cell) and either treated with TNFα/CHX at 3 hpi and 6 hpi or not treated at all. At 20 hpi, cells were stained with Hoechst DNA dye and observed by phase-contrast and florescence microscopy to visualize cellular and nuclear morphologies (Fig. 4).

Untreated and CHX-treated mock-infected cells appeared flat, elongated, and their nuclei appeared round (Fig. 4, panels 1, 3 and 2, 4) while close to 100% of those treated with TNFα/CHX displayed morphologies characteristic of apoptosis, including cell shrinkage, membrane blebbing (panel 5), and chromosome condensation (panel 6). HSV-1(F)- and HSV-2(G)-infected cells displayed cytopathic effect due to infection; however, these cells did not appear apoptotic (compare panels 7, 8 and 13, 14 with panels 5, 6). When TNFα/CHX was added at 3 hpi to HSV-1(F)- and HSV-2(G)-infected cells, the number of cells that appeared apoptotic increased dramatically (panels 9, 10 and 15, 16); HSV-2(G) plus CHX at 3 hpi had 79% cells with condensed chromatin compared to 5% in the untreated infection. The numbers of apoptotic cells decreased when TNFα/CHX was added at 6 hpi to infected cells (panels 11, 12 and 17, 18); 26% of HSV-2(G)-infected cells had condensed chromatin. These results suggest that HSV-2(G) can prevent TNFα/CHX-induced apoptosis in a manner similar to that of HSV-1.

To biochemically confirm these findings, whole cell extracts were prepared from the cells described above. Cells were harvested at 21 hpi, separated on a denaturing gel, transferred to nitrocellulose, and immunoblots were performed using anti-ICP4, anti-α-tubulin (Fig. 5A), anti-PARP, and anti-caspase-3 (Fig. 5B) antibodies. α-Tubulin was used as loading control to ensure equal protein concentration in each lane. The maximum amounts of

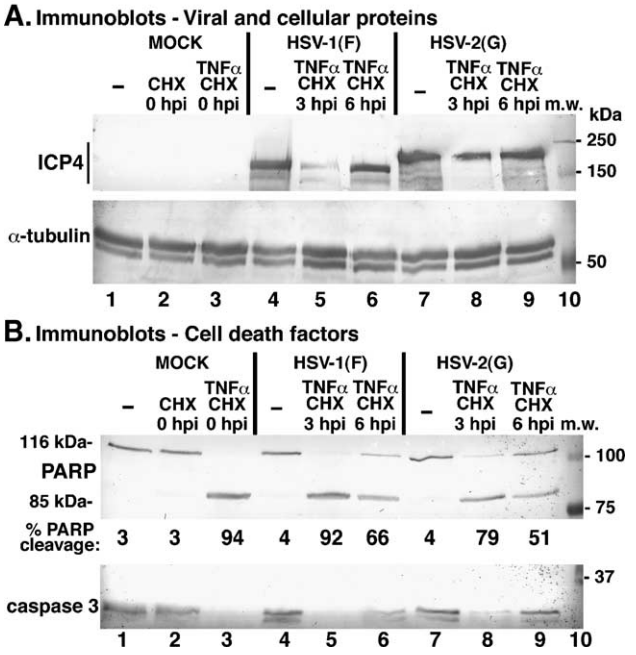


Fig. 5. HSV-2(G) prevention of TNFα/CHX-dependent apoptotic death factor processing. Whole cell extracts were prepared at 20 hpi from mock-, HSV-1(F)-, and HSV-2(G)-infected cells (MOI of 10 PFU/cell), separated on a denaturing gel, transferred to nitrocellulose, and probed with anti-ICP4, anti-α-tubulin (A), anti-PARP, and anti-caspase-3 (B) antibodies. Cells were either treated with CHX (10 μg/μl), TNFα/CHX (10 μg/μl) treated, or not treated at all (−) at the indicated times. Percentage of PARP cleavage was determined by NIH Image. Locations of molecular mass (kDa) markers are indicated in the margins.

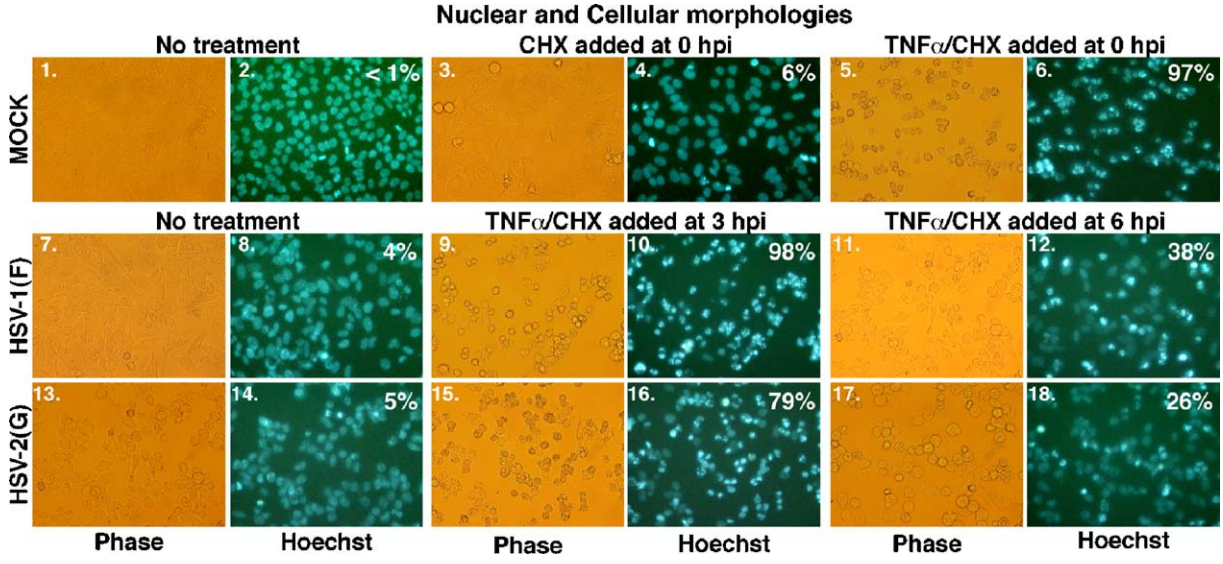


Fig. 4. HSV-2(G) prevention of TNFα/CHX-dependent apoptotic morphologies. HEp-2 cells were mock, HSV-1(F), and HSV-2(G) infected (MOI of 10 PFU/cell) for 19 h. Cells were treated with either CHX (10 μg/μl), TNFα/CHX (10 μg/μl), or not at all at the times indicated. Nuclear and cellular morphologies were visualized using fluorescence (Hoechst H33258) and phase-contrast microscopy (magnification, ×40). White numbers in the right corners correspond to the number of apoptotic cells.

ICP4, used as a viral marker to show that productive infection had occurred, were seen in non-treated cells (Fig. 5A, lanes 4 and 7). ICP4 levels significantly decreased when TNFα/CHX was added at 3 hpi (lanes 5 and 8) and they approached non-treated levels when TNFα/CHX was added at 6 hpi (lanes 6 and 9). Mock-infected cells in the absence or presence of CHX showed no PARP cleavage except background (3%) levels (Fig. 5B, lanes 1 and 2). The addition of TNFα/CHX to mock-infected cells resulted in almost complete (94%) PARP cleavage (lane 3).

PARP cleavage in HSV-1- and HSV-2-infected cells in the absence of treatment revealed only background levels (4%) comparable to mock (Fig. 5B, compare lanes 4 and 7 with lane 1). When TNFα/CHX was added at 3 hpi to HSV-1- and HSV-2-infected cells, PARP cleavage significantly increased (92% and 79%, respectively), resembling that of mock-infected cells treated with TNFα/CHX (compare lanes 5 and 8 with lane 3). Under these conditions, there was also complete disappearance of caspase-3 (lanes 3, 5, and 8). The maximum amount of PARP cleavage observed for the 3-hpi treatment with HSV-2(G) was not as high as that with HSV-1(F). This difference is similar to that observed in Fig. 1B with CHX treatment at 3 hpi and may suggest that HSV-1 is a more potent inducer of apoptosis than HSV-2. The amount of PARP and caspase-3 processing decreased when TNFα/CHX was added at 6 hpi in HSV-1 (92–66% PARP cleavage)- and HSV-2 (79–51% PARP cleavage)-infected cells. Taking these observations together, we can conclude that HSV-2(G) is able to prevent apoptosis induced by TNFα/CHX and the infected cell proteins required for this effect are synthesized between 3 and 6 hpi. This time frame corresponds to the HSV-2(G) apoptosis prevention window (Fig. 3).

### *NF-κB localization to nuclei during HSV-2(G) infection requires infected cell proteins synthesized prior to 6 hpi and correlates with apoptosis prevention*

The nuclear localization of the transcriptional regulatory factor NF-κB during HSV-1 infection has been extensively studied (Amici et al., 2001; Goodkin et al., 2003; Patel et al., 1998). We wished to examine the nuclear localization of NF-κB in HSV-2-infected HEp-2 cells using indirect immunofluorescence and immunoblotting techniques. Initially, HEp-2 cells were mock-, HSV-1(F)-, and HSV-2(G)-infected (MOI = 10), treated with CHX at 3, 6 hpi, or left untreated and, at 8 hpi, fixed with formaldehyde/acetone for indirect immunofluorescence analyses as described in Materials and methods. Cells were double stained with a monoclonal antibody against NF-κB plus a polyclonal antibody specific for the IE viral protein ICP22 of HSV-1 and HSV-2 (Blaho et al., 1997). The results (Fig. 6) were as follows.

NF-κB remained in the cytoplasm of mock-infected cells in the absence and presence of CHX (Fig. 6, panels 1 and 3). When control TNFα/CHX was added to mock-infected cells, NF-κB was found mainly in nuclei (panel 5), as expected (Beg et al., 1993; Goodkin et al., 2003; Wallach et al., 1999). At 8 hpi following HSV-2(G) infection alone, numerous cells showed nuclear NF-κB staining; the most intensely stained cells (panel 13) were those that also had high levels of nuclear ICP22 (panel 14). While CHX addition at 3 hpi did not yield a significant decrease in the levels of ICP22 in infected cells (panel 16), all NF-κB was cytoplasmic (panel 15). When CHX was added at 6 hpi, NF-κB was detected in the nuclei to the same extent as those infected cells in the absence of CHX (compare panels 17 and 13). These results imply that HSV-2(G)-infected cell

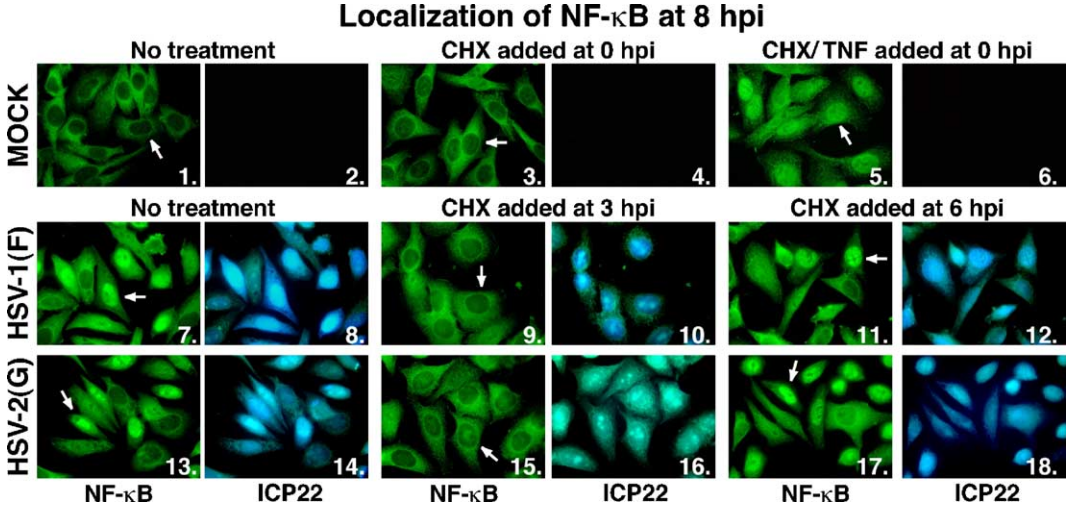


Fig. 6. HSV-2(G) infection induces NF-κB nuclear localization. HEp-2 cells seeded on coverslips were mock, HSV-1(F), and HSV-2(G) infected (MOI of 10 PFU/cell), fixed for indirect immunofluorescence at 8 hpi, and double stained with monoclonal anti-NF-κB and polyclonal anti-ICP22 antibodies. HEp-2 cells were either treated with CHX (10 μg/μl) or TNFα/CHX (10 μg/μl) at the times indicated. NF-κB and ICP22 were observed with FITC- and AMCA-conjugated secondary antibodies, respectively. Arrows mark representative localizations of NF-κB (magnification, ×100).

proteins produced at 3 hpi are not sufficient to stimulate NF-κB.

To biochemically confirm these results and to assess apoptotic status, HEp-2 cells were infected and treated as above but at 22 hpi, cells were harvested, nuclear and cytoplasmic extracts were prepared, separated on a denaturing gel, transferred to nitrocellulose, and probed with anti-ICP4 (Fig. 7A), anti-NF-κB (Fig. 7B), anti-PARP, anti-caspase-3 (Fig. 7C) antibodies. To ensure that contamination of the subcellular fractions did not occur, the immunoblot was also probed for α-tubulin (cytoplasmic marker) and Lamin B (nuclear marker). These proteins were detected exclusively in their respective lanes (data not shown); the only exception was that low levels of α-tubulin were found in the nuclear lane of mock-infected cells treated with TNFα/CHX, presumably due to extensive cell death occurring in these cells (Morton and Blaho, unpublished results).

ICP4 predominated in nuclei and its level decreased when CHX was added at 3 hpi (Fig. 7A, lane 14) compared to no treatment (lane 12) or when CHX was added at 6 hpi (lane 16). In the absence of treatment, infection with HSV-2(G) resulted in more NF-κB in the nuclear fraction than the cytoplasmic fraction (Fig. 7B, lanes 12 and 13). When CHX was added at 3 hpi, the majority of NF-κB remained in the cytoplasmic fraction (lane 15). The addition of CHX at 6 hpi revealed an equal, if not greater, amount of NF-κB in the nuclear than in the cytoplasmic fractions (lanes 16 and 17). This behavior in HSV-2(G)-infected cells was similar to that observed with HSV-1(F) (lanes 6–11). Based on these results, we conclude that NF-κB translocates to nuclei during HSV-2(G) infection and infected cell proteins synthesized after 3 hpi are needed for this to occur.

The indirect immunofluorescence experiments above (Fig. 6) were performed prior to a time when the cells would show features of apoptosis. To investigate cellular death factor processing and nuclear localization of NF-κB, we also probed the immunoblot (Figs. 7A and B) for PARP and caspase-3. Finally, phase-contrast microscopic images were documented prior to harvesting the cells (Fig. 7D). As expected, mock-infected cells in the absence of treatment revealed no PARP cleavage or caspase-3 activation (Fig. 7C, lanes 2 and 3). In contrast, mock-infected cells treated with TNFα/CHX showed almost 100% PARP cleavage, complete activation of caspase-3 (lanes 4 and 5), and showed apoptotic cell morphologies (Fig. 7D). HSV-2(G)-infected cells in the absence of CHX showed only background levels of PARP cleavage, relatively no caspase-3 processing (lanes 12 and 13), and non-apoptotic CPE (Fig. 7D). The addition of CHX at 3 hpi to HSV-2(G)-infected cells resulted in significant PARP cleavage and enhanced caspase-3 activation (lane 15), while processing of these factors was reduced when CHX was added at 6 hpi (lane 17). Accordingly, the 6-hpi CHX addition showed less apoptotic morphologies with

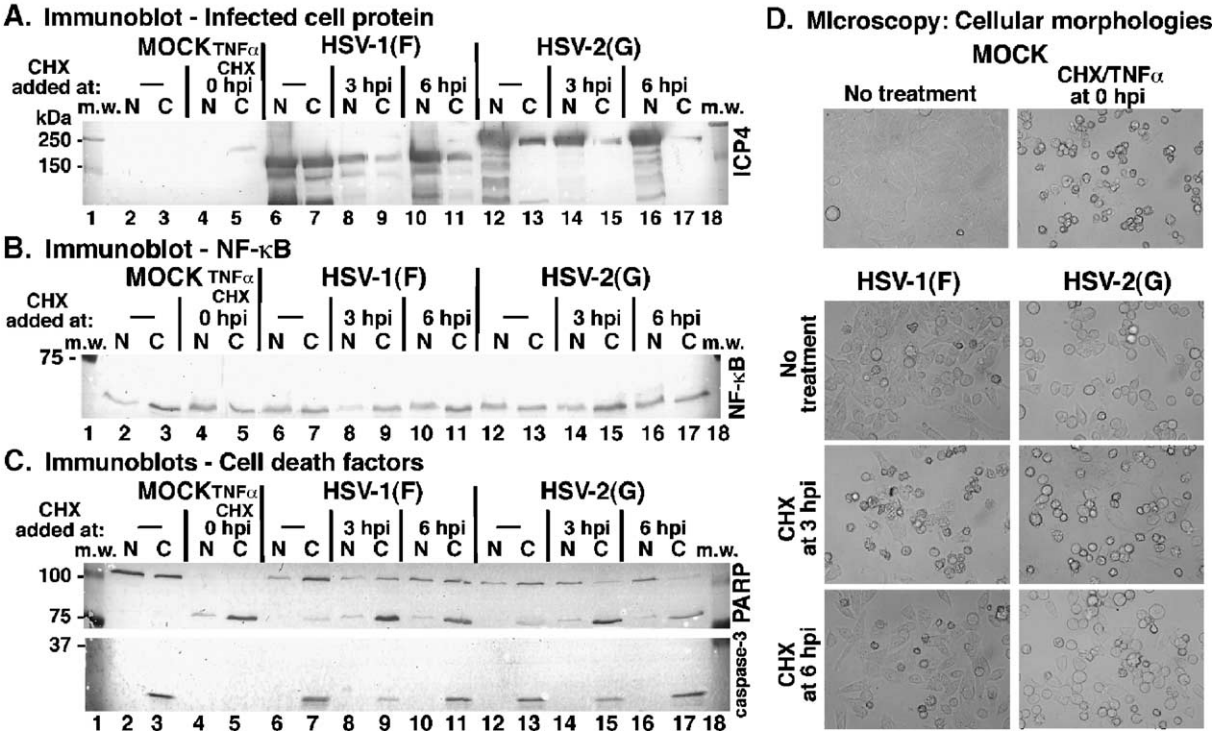


Fig. 7. NF-κB partitioning in nuclear fractions correlates with apoptosis prevention during HSV-2(G) infection. HEp-2 cells were mock infected or infected with HSV-1(F) or HSV-2(G) (MOI of 10 PFU/cell), harvested at 20 hpi, nuclear and cytoplasmic fractions were prepared, separated in a denaturing gel, transferred to nitrocellulose, and probed with anti-ICP4 (A), anti-NF-κB (B), anti-PARP, and anti-caspase-3 (C) antibodies. Cells were treated with CHX (10 μg/μl), TNFα/CHX (10 μg/μl), or not at all (−) at the times indicated. Locations of molecular mass (kDa) markers are indicated in the margins. Prior to harvesting, infected cell morphologies (D) were visualized by phase-contrast microscopy (magnification, ×40).

HSV-2(G) than the 3-hpi addition (Fig. 7D). Thus, when cell death was maximum (Fig. 7C, lane 15), NF-κB was cytoplasmic (Fig. 7B, lane 15). When apoptosis was prevented by the virus, either without treatment (Fig. 7C, lane 13) or with the 6-hpi CHX addition (Fig. 7C, lane 17), NF-κB was detected in nuclei (Fig. 7B, lanes 12 and 16). Taken together, these results indicate that nuclear translocation of NF-κB during HSV-2(G) infection correlates with apoptosis prevention. As similar conclusion was drawn for HSV-1 infection (Goodkin et al., 2003; Gregory et al., 2004).

*Apoptosis modulation by HSV-2 clinical isolates*

All of the results above were obtained using the laboratory HSV-2(G) strain. It has been reported that laboratory-adapted strains of HSV-2 had weaker anti-apoptotic capability against certain environmental agents than HSV-1 (Jerome et al., 1998) and primary clinical isolates showed no inhibitory activity (Jerome et al., 2001). Due to this issue of whether HSV-2 clinical isolates have the ability to induce or prevent apoptosis, we set out to determine (i) if apoptosis can occur in HEp-2 cells infected with HSV-2 clinical isolates and (ii) its extent when compared to HSV-1 and HSV-2 control viruses. HEp-2 cells were either mock infected or infected (MOI = 10 PFU/cell) with HSV-1(F), HSV-1(TC), HSV-2(G), HSV-2(333), HSV-2(C2), or HSV-2(C9). TC is an HSV-1 clinical isolate, while C2 and C9 are HSV-2 clinical isolates. 333 was used as an alternative laboratory strain, for comparison to strain HSV-2(G). Infected cells were either treated with CHX at 3 hpi or not treated at all. At 19 hpi, cells were stained with Hoechst DNA dye and nuclear and cellular morphologies were visualized (Fig. 8).

Mock-infected cells in the absence and presence of CHX had oval nuclei (Fig. 8, panels 1 and 3) and appeared flat and elongated (panels 2 and 4). All infected cells in the absence of CHX displayed effects of cytopathic effect, appearing rounded (panels 6, 10, 14, 18, 22, 26) with evidence of chromatin margination (panels 5, 9, 13, 17, 21, 25); this latter feature was quite apparent with HSV-1(F). The extents of detectable chromatin condensation in these cells were less than 13%. The addition of CHX at 3 hpi resulted in cells displaying apoptotic characteristics including, chromatin condensation (panels 7, 11, 15, 19, 23, 27), membrane blebbing, and cell shrinkage (panels 8, 12, 16, 20, 24, 28). Both laboratory HSV-1(F) and the clinical isolate HSV-1(TC) had significant amounts of condensed chromatin (75% and 51%, respectively), while the two laboratory HSV-2 strains, G and 333, had equal amounts (66% and 70%). The two clinical HSV-2 strains, C2 and C9, had condensed chromatin levels similar to that of the other viruses (58 and 68%, respectively). These findings suggest that the capacity of the clinical virus isolates to induce apoptosis was similar to that of the laboratory strains.

To biochemically confirm these observations, whole cell extracts of the cells above were made at 20 hpi, separated on a denaturing gel, transferred to nitrocellulose. and probed with anti-ICP4, anti-α-tubulin (Fig. 9A), anti-PARP, and anti-caspase-3 (Fig. 9B) antibodies. High levels of ICP4 were detected in all virally infected cells in the absence of CHX addition, indicating productive infections. The levels of ICP4 were reduced by the addition of CHX at 3 hpi, confirming the inhibition of protein synthesis. Mock-infected cells with and without CHX did not show PARP cleavage above background (4% and 6% cleavage) levels (Fig. 9, lanes 2 and 3). In the absence of CHX, infected cells did not exhibit PARP cleavage above 17%. While HEp-2 cells infected with HSV-2 clinical isolates C2 and C9 showed minimal PARP and caspase-3 cleavage in the absence of CHX (lanes 12 and 15), the addition of CHX at 3 hpi caused the amount of apoptosis to increase approximately four-fold (lanes 13 and 14). Importantly, the PARP processing and caspase-3 activation observed with C2 (63%) and C9 (66%) plus CHX was equivalent to that of the HSV-2 laboratory strains, G (64%) and 333 (69%) (compare lanes 13, 14 with lanes 9, 11). Thus, we conclude that HSV-2 clinical and laboratory strains are able to induce and then prevent apoptosis in infected HEp-2 cells in the same manner.

## Discussion

While the details of apoptosis during HSV-1 infection have become more defined in recent years, issues regarding the association of HSV-2 with the programmed cell death process remain unresolved. Our goal was to directly test whether HSV-2 could modulate apoptosis during its productive replication cycle. Our key findings may be summarized as follows.

*HSV-2 first triggers and then prevents apoptosis during productive infection*

This conclusion is based on the observation that significant apoptosis occurs during HSV-2 infection if CHX is added at 3 hpi but not if the drug is added at 6 hpi. This implies that upon infection, the cells begin the concerted cascade of apoptosis, and if the appropriate anti-apoptotic proteins are not synthesized, cell death occurs. We observed this effect with two laboratory strains, HSV-2(G) and HSV-2(333), as well as with two HSV-2 and one HSV-1 clinical isolates. That there was a significant decrease in the number of cells that died of apoptosis when CHX is added at 6 hpi demonstrates that proteins needed to prevent apoptosis were synthesized prior to that time. Our detailed time course of CHX addition experiment demonstrated that proteins produced in a window between 3 and 5 h of HSV-2 infection are required for blocking virus-induced cell death. Thus, these studies show that HSV-2 has the ability to

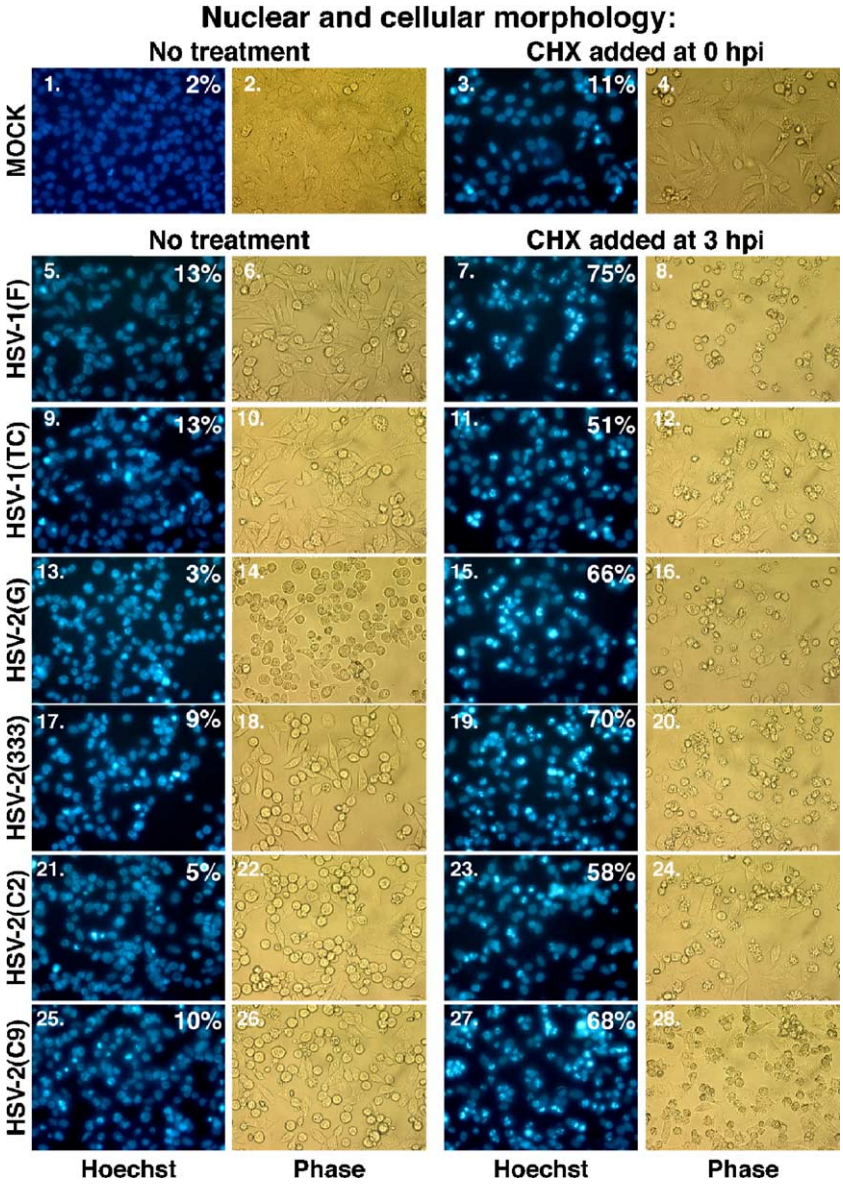


Fig. 8. Nuclear and cellular morphologies of cells infected with clinical HSV-2 isolates. HEp-2 cells were infected with HSV-1(F), HSV-2(G), HSV-2(333), and clinical isolates HSV-1(TC), HSV-2(C2), HSV-2(C9) (MOI of 10 PFU/cell), or mock infected. Cells were either treated (+) with CHX (10 μg/μl) at 3 hpi or not at all. At 19 hpi, cells were visualized using fluorescence (Hoechst H33258) and phase-contrast microscopy (magnification, ×40). White numbers in the right corners correspond to the number of apoptotic cells. Locations of molecular mass (kDa) markers are indicated in the margins.

induce and then prevent apoptosis in HEp-2 cells and this ability mirrors that of HSV-1 (Aubert et al., 1999).

It is perhaps not surprising that HSV-2 ends up being able to block apoptosis in a manner similar to HSV-1 since the genomes of these viruses are colinear and most viral gene products can functionally substitute for one another between the two strains (Blaho et al., 1994; Conley et al., 1981; Knipe et al., 1978, 1981; Morse et al., 1978; Pereira et al., 1977). Thus, it seems intuitive that viral anti-apoptotic proteins would likely be similar between HSV-1 and HSV-2. Consistent with this idea are the reports of the HSV-2 $U_S3$ protein having anti-apoptotic activity (Asano et al., 1999; Hata et al., 1999). In addition, the R1 subunit of the HSV-2 ribonucleotide reductase has been described to be anti-apoptotic (Langelier et al., 2002; Perkins et al., 2003) and one study has reported that HSV-1 strains deleted for ICP6 have enhanced apoptosis (Langelier et al., 2002). However, ICP6 is expressed very early during HSV-1 infection and the impact of its loss on late viral protein accumulation could explain this effect.

### *NF-κB translocates to nuclei of HSV-2-infected HEp-2 cells*

Upon determining that the HSV-2 and HSV-1 apoptosis prevention windows were the same, we tested whether the HSV-2-infected cell proteins produced in that time frame could block external, environmentally stimulated apoptosis. We observed that HSV-2 blocked cell death triggered by

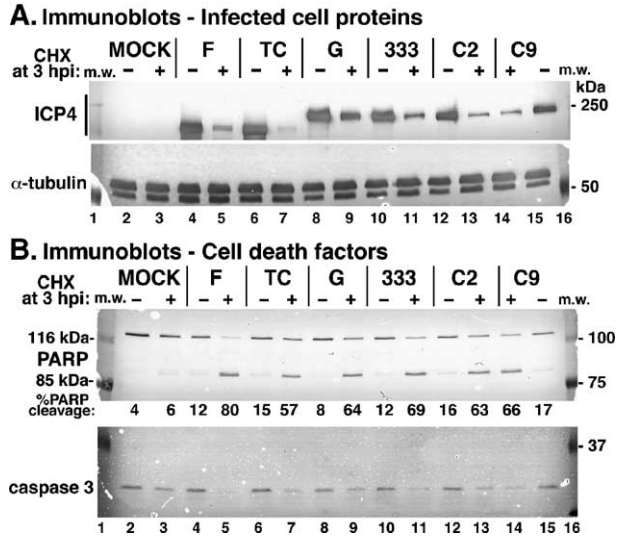


Fig. 9. Death factor processing in cells infected with clinical HSV-2 isolates. HEp-2 cells were infected with HSV-1(F), HSV-2(G), HSV-2(333), and clinical isolates HSV-1(TC), HSV-2(C2), or HSV-2(C9) (MOI of 10 PFU/cell). At 3 hpi, cells were untreated (−) or CHX (10 μg/μl) was added (+) and whole cell extracts were prepared at 20 hpi, separated in a denaturing gel, transferred to nitrocellulose, and probed with anti-ICP4, anti-α-tubulin (A), anti-PARP, and anti-caspase-3 (B) antibodies. Percentage of PARP cleavage was determined by NIH Image.

TNFα plus CHX. Based on this finding, we predict that HSV-2 likely blocks other environmental pro-apoptotic stimuli. In response to TNFα treatment, the cellular transcription factor NF-κB becomes activated and translocates to the nucleus where it regulates genes which contribute to the cell's survival (Beg and Baltimore, 1996; Beg et al., 1993; Wallach et al., 1999). We observed that NF-κB was detected in nuclei of HSV-2-infected cells. In addition, the presence of NF-κB in infected cell nuclei correlated with apoptosis prevention. That NF-κB was not nuclear in HSV-2-infected cells when protein translation was blocked at 3 hpi suggests that early infected cell protein synthesis is required for NF-κB activation. Similar observations have been made during HSV-1 infection (Amici et al., 2001; Goodkin et al., 2003; Medici et al., 2003; Patel et al., 1998). In the case of HSV-1, NF-κB activation appears to serve a pro-survival function to ensure productive viral replication (Gregory et al., 2004). Thus, it is likely that NF-κB provides a similar function during HSV-2 infection. Experiments are currently under way to determine whether the inhibition of nuclear NF-κB reduces the apoptosis suppression capability of HSV-2.

### *The induction of apoptosis by HSV-2 differs from that of HSV-1*

The most interesting observation we made was that maximum apoptosis with HSV-2 was detected when we blocked protein translation at 3 hpi. It is important to note that apoptotic features were detected when translation was prevented at 0 and 1 hpi, but these levels were consistently less than that at 3 hpi. One explanation for this is that at these early times, HSV-2 may not be as potent an apoptotic inducer as HSV-1. Numerous pieces of evidence argue that HSV-1 immediate early gene expression is required to trigger apoptosis (Aubert et al., 1999; Sanfilippo et al., 2004). If this is also the case for HSV-2, one possible explanation could be that the level of HSV-2 IE gene expression is less than that of HSV-1 in these cells. However, earlier findings that HSV-2 replication occurs more rapidly and IE protein accumulate to higher levels than HSV-1 in HeLa cells seem to argue against this idea (Blaho and Roizman, 1991; Blaho et al., 1994). Another consideration is the fact that HSV-2 has a more potent virion host shutoff effect than HSV-1 (Fenwick and Walker, 1978; Fenwick et al., 1979). However, at least under the conditions utilized in this study, we did not observe any distinctions between the replication efficiencies of HSV-1 and HSV-2 in our HEp-2 cells. An alternative explanation is that HSV-2 requires the de novo synthesis of infected cell protein for optimal apoptosis while HSV-1 does not. This is an intriguing notion and would represent the first significant difference in apoptosis modulation between HSV-2 and HSV-1. The development of appropriate biochemical and molecular genetic systems should allow the determination of the molecular basis of the difference in apoptosis induction between HSV-2 and HSV-1.

## Methods and materials

### *Cells and viruses*

All cells were maintained and passaged in Dulbecco's modified Eagle's medium (DMEM) supplemented with 5% fetal bovine serum. Human epithelial (HEp-2) and African green monkey kidney (Vero) cells were obtained from the American Type Culture Collection. The wild-type viruses HSV-1(F) and HSV-2(G) were provided by Bernard Roizman, University of Chicago. The clinical strain HSV-1(TC) was isolated (Bowles et al., 2005) and provided by Robert Bowles, MSSM, while clinical isolates HSV-2(C2), HSV-2(C9), and the laboratory strain HSV-2(333) were provided by Betsy Herold, MSSM. To obtain virus stocks, subconfluent Vero monolayer cells (approximately $2 \times 10^6$) were inoculated with virus at a multiplicity of infection (MOI) of 0.01 for 2 h at 37 °C in 199 V medium (Life Technologies) supplemented with 1% newborn calf serum (NBCS). The inoculum was removed, fresh DMEM supplemented with 5% NBCS was added, the cells incubated for 2–3 days at 37 °C in 5% $CO_2$. Virus stocks were prepared once the infection had reached 100% cytopathic effect, the titer was determined on Vero cells, and aliquots of virus stored at −80 °C. Detailed previous studies have demonstrated the induction of HSV-dependent apoptosis is not due to contaminants present in virus stock preparations (Sanfi-

lippo et al., 2004). All MOIs were derived from the number of plaque-forming units (PFU) of virus on Vero cells.

*Preparation of whole cell extracts*

Infected cells were harvested by scraping them off the dish directly into the medium. After centrifugation for 5 min at 1000 × *g*, cell pellets were rinsed and resuspended in phosphate-buffered saline (PBS) containing a 10-μM concentration of the following protease inhibitors (all obtained from Sigma): *N*-tosyl-L-phenyl-alanine-chloromethylketone (TPLK), phenylmethylsulfonyl fluoride (PMSF), and tosyl-L-lysine-chloromethylketone (TLCK). Infected cells were disrupted by sonication on ice three times for 10 s at an output of 2 with a Branson sonifier. The protein concentration of each sample was determined by a modified Bradford protein assay as recommended by the manufacturer (BioRad).

*Denaturing gel electrophoresis and immunoblotting technique*

Approximately 50 μg of infected cell protein from whole cell extracts or subcellular fractions were electrophoretically separated in a 15% sodium dodecyl sulfate–polyacrylamide gel cross-linked with *N*,*N*′-diallytartardiamide (Blaho and Roizman, 1998), electrically transferred to nitrocellulose using a tank apparatus (BioRad), and blocked in 5% milk in PBS for a minimum of 1 h. Blots were probed with appropriate primary antibodies (described below) for a minimum of 1 h. Secondary goat anti-mouse or anti-rabbit antibodies conjugated to alkaline phosphatase (obtained from Southern Biotechnology) was then added for 1 h prior to colorimetric development. Prestained protein molecular weight markers (purchased from BioRad) were included on all gels. Immunoblots were digitized (600–800 dots/in.) with an AGFA Arcus II scanner. Raw digital images were saved as TIFF image files with Adobe Photoshop and organized into figures with Adobe Illustrator.

*Immunological reagents*

The antibodies used to detect viral and cellular proteins were the following. RGST22 is a rabbit polyclonal antibody specific for ICP22 (Blaho et al., 1997). H114 is a mouse monoclonal antibody specific for ICP4 (Goodwin Institute for Cancer Research). Mouse monoclonal antibody DM-A1 that is specific for α-tubulin was obtained from Sigma. Mouse monoclonal antibodies specific for caspase-3 and PARP were obtained from Santa Cruz Biotechnology, Inc. Mouse monoclonal antibody for NF-κB is generated against the p65 subunit and was obtained from Santa Cruz Biotechnology, Inc. Polyclonal goat antibody specific for Lamin B was purchase from Santa Cruz Biotechnology, Inc. All primary antibodies used for immunoblotting were used at a dilution of 1:1000 in 1% BSA. Alkaline phosphatase-conjugated goat anti-rabbit or anti-mouse secondary antibodies were purchased from Southern Biotech, Inc. and used at 1:1000 dilutions in 1% BSA. Fluorescein isothiocyanate (FITC)-conjugated anti-mouse IgG (H + L) was purchased from Vector Laboratories (Santa Cruz, CA) and used at dilutions of 1:300 in 1% BSA. AMCA anti-rabbit IgG (H + L) was purchased from Vector Laboratories and used at a 1:300 dilution in 1% BSA.

*Biochemical and pharmacological reagents: use of CHX and TNFα*

CHX addition at the time of HSV-1 infection inhibits infected cell protein synthesis, leading to apoptosis of human HEp-2 cells (Aubert and Blaho, 1999; Goodkin et al., 2004; Koyama and Adachi, 1997). CHX (10 μg/ml) was added to the media of infected cells and maintained until the cells were harvested. As a positive control for apoptosis, CHX (10 μg/ml) and TNFα (10 μg/ml) were added to mock-infected HEp-2 cells. Lyophilized TNFα (Sigma) was dissolved in sterile PBS containing 1% BSA and aliquots were stored at −80 °C.

*DNA laddering assay*

Nucleosomal cleavage of cellular DNA was assessed essentially as described (Aubert and Blaho, 1999). Cells were scraped into the medium and collected by centrifugation for 5 min at 1000 × *g*. The cells were rinsed with ice cold phosphate–saline buffer (PBS) and centrifuged again to form a cellular pellet. Cells were lysed by resuspending the pellet in 400 μl of TE (10 mM Tris–HCl, pH 8.0, 10 mM EDTA) containing 0.6% SDS and then mixed with 125 μl of 5 M NaCl. After overnight incubation at 4 °C (to extract the DNA), the solution was centrifuged for 25 min at 12,000 × *g* to precipitate chromosomal DNA. The supernatant was collected and sequentially subjected to digestion with 0.1 mg/ml RNAse A (37 °C for 1 h) and 1 mg/ml proteinase K (50 °C for 2 h), followed by standard phenol/chloroform extractions and ethanol precipitation. DNA was precipitated overnight at −80 °C and samples were centrifuged at 12,000 × *g* for 20 min. The precipitated DNA was separated in a standard 1.5% Tris–borate–EDTA agarose gel containing 0.1 μg/ml ethidium bromide and visualized using UV illumination.

*Quantitation of cells with condensed chromatin and processed death factors*

Live cells were stained at 17 hpi with Hoechst 33258 dye (Sigma) at a concentration of 5 μg/ml for 30 min at 37 °C. Cells with condensed chromatin (visualized by fluorescence microscopy) as well as the total number of cells were counted; approximately 150 total cells were counted for each treatment group. The percentage of apoptotic cells was calculated as follows: (number of apoptotic cells /

number of total cells in the field) × 100. Live cells were observed with an Olympus IX70/IX-FLA inverted fluorescent microscope and images were acquired using a Sony DKC-5000 digital photo camera at a resolution of 600–800 dots/in. linked to a PowerMac and processed through Adobe Photoshop.

During the execution phase of apoptosis, full-length PARP (116 kDa) is cleaved and the inactive form of caspase-3 (procaspase-3) becomes cleaved (Aubert et al., 1999). The PARP antibody used in our study reacts with both the full-length form and its 85-kDa cleavage product. While our caspase-3 antibody recognizes the uncleaved form (32 kDa) and one of the processed forms (20 kDa), under our gel electrophoresis conditions, only the uncleaved (inactive) form is resolved. Therefore, the loss of caspase-3 reactivity corresponds to apoptosis induction in our system (Aubert et al., 1999). PARP cleavage was quantitated as described (Aubert et al., 2001; Nguyen et al., 2005) using the public domain NIH Image computer application (developed at the National Institutes of Health and available on the Internet at http://www.rsb.info.nih.gov/nih-image). Integrated densities (ID) of the 116,000 mol. wt. uncleaved and 85,000 mol. wt. cleaved PARP were determined and % PARP cleavage was calculated using the following formula: % cleaved = {(cleaved PARP ID) / (cleaved PARP ID plus uncleaved PARP ID)}. Each experiment was performed at least two times.

*Indirect immunofluorescence*

HEp-2 cells were prepared for indirect immunofluorescence as previously described (Pomeranz and Blaho, 1999; Yedowitz et al., 2005). Briefly, cells were rinsed twice with non-sterile PBS, fixed in 2.5% methanol-free formaldehyde (Polysciences, Inc.) for 20 min at room temperature. Cells were again rinsed twice with PBS and permeablized with 100% acetone at −20 °C for 4 min. Cells were rinsed with PBS and incubated overnight with 1% BSA supplemented with 10 μg of pooled human immunoglobulin (Ig; Sigma) per ml. Treatment with Ig was previously shown to sufficiently neutralize Fc binding by the viral gE and gI proteins (Kotsakis et al., 2001). Primary antibodies used for indirect immunofluorescence were diluted and added for 1 h; mouse monoclonal NF-κB antibody and rabbit polyclonal ICP22 were both diluted 1:500. After rinsing twice with PBS, the appropriate secondary antibody was added to the cells and incubated for 45 min in the dark. After the cells were again rinsed twice with PBS, they were preserved with Prolong Antifade (Molecular Probes) as an anti-bleaching agent, mounted on a fresh glass slide, and stored at 4 °C for at least 4 h. Cells were visualized on an Olympus IX70/IX-FLA inverted fluorescence microscope and images were acquired at a resolution of 600–800 dots/in. using a Sony DKC-5000 digital photo camera linked to a PowerMac. Raw digital images were saved as tagged image files (TIF) with Adobe Photoshop, organized into figures with Adobe Illustrator.

## Acknowledgments

We thank Elise Morton for expert cell culture technical assistance and developing the lamin/tubulin immunological system for confirming the integrity of subcellular fractions, as well as Betsy Herold (MSSM-Pediatrics) for assistance in obtaining primary virus isolates. These studies were supported by a grant from the U.S. Public Health Service (AI 48582).

## References

Amici, C., Belardo, G., Rossi, A., Santoro, M.G., 2001. Activation of I kappa b kinase by herpes simplex virus type 1. A novel target for anti-herpetic therapy. J. Biol. Chem. 276 (31), 28759–28766.

Asano, S., Honda, T., Goshima, F., Watanabe, D., Miyake, Y., Sugiura, Y., Nishiyama, Y., 1999. US3 protein kinase of herpes simplex virus type 2 plays a role in protecting corneal epithelial cells from apoptosis in infected mice. J. Gen. Virol. 80 (Pt. 1), 51–56.

Aubert, M., Blaho, J.A., 1999. The herpes simplex virus type 1 regulatory protein ICP27 is required for the prevention of apoptosis in infected human cells. J. Virol. 73 (4), 2803–2813.

Aubert, M., Blaho, J.A., 2001. Modulation of apoptosis during herpes simplex virus infection in human cells. Microbes Infect. 10, 859–866.

Aubert, M., O'Toole, J., Blaho, J.A., 1999. Induction and prevention of apoptosis in human HEp-2 cells by herpes simplex virus type 1. J. Virol. 73 (12), 10359–10370.

Aubert, M., Rice, S.A., Blaho, J.A., 2001. Accumulation of herpes simplex virus type 1 early and leaky-late proteins correlates with apoptosis prevention in infected human HEp-2 cells. J. Virol. 75 (2), 1013–1030.

Beg, A.A., Baltimore, D., 1996. An essential role for NF-kappaB in preventing TNF-alpha-induced cell death. Science 274 (5288), 782–784.

Beg, A.A., Finco, T.S., Nantermet, P.V., Baldwin, A.S. Jr., 1993. Tumor necrosis factor and interleukin-1 lead to phosphorylation and loss of I kappa B alpha: a mechanism for NF-kappa B activation. Mol. Cell. Biol. 13 (6), 3301–3310.

Blaho, J.A., Roizman, B., 1991. ICP4, the major regulatory protein of herpes simplex virus, shares features common to GTP-binding proteins and is adenylated and guanylated. J. Virol. 65 (7), 3759–3769.

Blaho, J.A., Roizman, B., 1998. Analyses of HSV proteins for posttranslational modifications and enzyme functions. In: Brown, S.M., Maclean, A.R. (Eds.), Methods in Molecular Medicine: Herpes Simplex Virus Protocols, vol. 10. Human Press, Inc., Totowa, pp. 237–256.

Blaho, J.A., Mitchell, C., Roizman, B., 1994. An amino acid sequence shared by the herpes simplex virus 1 alpha regulatory proteins 0, 4, 22, and 27 predicts the nucleotidylylation of the UL21, UL31, UL47, and UL49 gene products. J. Biol. Chem. 269 (26), 17401–17410.

Blaho, J.A., Zong, C.S., Mortimer, K.A., 1997. Tyrosine phosphorylation of the herpes simplex virus type 1 regulatory protein ICP22 and a cellular protein which shares antigenic determinants with ICP22. J. Virol. 71 (12), 9828–9832.

Bowles, R., Yedowitz, J.C., Blaho, J.A., 2005. Unpublished results.

Conley, A.J., Knipe, D.M., Jones, P.C., Roizman, B., 1981. Molecular genetics of herpes simplex virus: VII. Characterization of a temperature-sensitive mutant produced by in vitro mutagenesis and defective in DNA synthesis and accumulation of gamma polypeptides. J. Virol. 37 (1), 191–206.

Fenwick, M.L., Walker, M.J., 1978. Suppression of the synthesis of cellular macromolecules by herpes simplex virus. J. Gen. Virol. 41 (1), 37–51.

Fenwick, M., Morse, L.S., Roizman, B., 1979. Anatomy of herpes simplex virus DNA: XI. Apparent clustering of functions effecting rapid inhibition of host DNA and protein synthesis. J. Virol. 29 (2), 825–827.

Fleck, M., Mountz, J.D., Hsu, H.C., Wu, J., Edwards, C.K., Kern, E.R., 1999. Herpes simplex virus type 2 infection induced apoptosis in peritoneal macrophages independent of Fas and tumor necrosis factor-receptor signaling. Viral Immunol. 12 (3), 263–275.

Galvan, V., Roizman, B., 1998. Herpes simplex virus 1 induces and blocks apoptosis at multiple steps during infection and protects cells from exogenous inducers in a cell-type-dependent manner. Proc. Natl. Acad. Sci. U.S.A. 95 (7), 3931–3936.

Goodkin, M.L., Ting, A.T., Blaho, J.A., 2003. NF-kappaB is required for apoptosis prevention during herpes simplex virus type 1 infection. J. Virol. 77 (13), 7261–7280.

Goodkin, M.L., Morton, E.R., Blaho, J.A., 2004. Herpes simplex virus infection and apoptosis. Int. Rev. Immunol. 23 (1–2), 141–172.

Gregory, D., Hargett, D., Holmes, D., Money, E., Bachenheimer, S.L., 2004. Efficient replication by herpes simplex virus type 1 involves activation of the IkappaB kinase-IkappaB-p65 pathway. J. Virol. 78 (24), 13582–13590.

Hata, S., Koyama, A.H., Shiota, H., Adachi, A., Goshima, F., Nishiyama, Y., 1999. Antiapoptotic activity of herpes simplex virus type 2: the role of US3 protein kinase gene. Microbes Infect. 1 (8), 601–607.

Jerome, K.R., Tait, J.F., Koelle, D.M., Corey, L., 1998. Herpes simplex virus type 1 renders infected cells resistant to cytotoxic T-lymphocyte-induced apoptosis. J. Virol. 72 (1), 436–441.

Jerome, K.R., Fox, R., Chen, Z., Sears, A.E., Lee, H., Corey, L., 1999. Herpes simplex virus inhibits apoptosis through the action of two genes, Us5 and Us3. J. Virol. 73 (11), 8950–8957.

Jerome, K.R., Fox, R., Chen, Z., Sarkar, P., Corey, L., 2001. Inhibition of apoptosis by primary isolates of herpes simplex virus. Arch. Virol. 146 (11), 2219–2225.

Jones, C.A., Fernandez, M., Herc, K., Bosnjak, L., Miranda-Saksena, M., Boadle, R.A., Cunningham, A., 2003. Herpes simplex virus type 2 induces rapid cell death and functional impairment of murine dendritic cells in vitro. J. Virol. 77 (20), 11139–11149.

Kerr, J.F., Wyllie, A.H., Currie, A.R., 1972. Apoptosis: a basic biological phenomenon with wide-ranging implications in tissue kinetics. Br. J. Cancer 26 (4), 239–257.

Knipe, D.M., Ruyechan, W.T., Roizman, B., Halliburton, I.W., 1978. Molecular genetics of herpes simplex virus: demonstration of regions of obligatory and nonobligatory identity within diploid regions of the genome by sequence replacement and insertion. Proc. Natl. Acad. Sci. U.S.A. 75 (8), 3896–3900.

Knipe, D.M., Batterson, W., Nosal, C., Roizman, B., Buchan, A., 1981. Molecular genetics of herpes simplex virus: VI. Characterization of a temperature-sensitive mutant defective in the expression of all early viral gene products. J. Virol. 38 (2), 539–547.

Kotsakis, A., Pomeranz, L.E., Blouin, A., Blaho, J.A., 2001. Microtubule reorganization during herpes simplex virus type 1 infection facilitates the nuclear localization of VP22, a major virion tegument protein. J. Virol. 75, 8697–8711.

Koyama, A.H., Adachi, A., 1997. Induction of apoptosis by herpes simplex virus type 1. J. Gen. Virol. 78 (Pt. 11), 2909–2912.

Koyama, A.H., Miwa, Y., 1997. Suppression of apoptotic DNA fragmentation in herpes simplex virus type 1-infected cells. J. Virol. 71 (3), 2567–2571.

Koyama, A.H., Akari, H., Adachi, A., Goshima, F., Nishiyama, Y., 1998. Induction of apoptosis in HEp-2 cells by infection with herpes simplex virus type 2. Arch. Virol. 143 (12), 2435–2441.

Koyama, A.H., Fukumori, T., Fujita, M., Irie, H., Adachi, A., 2000. Physiological significance of apoptosis in animal virus infection. Microbes Infect. 2 (9), 1111–1117.

Langelier, Y., Bergeron, S., Chabaud, S., Lippens, J., Guilbault, C., Sasseville, A.M., Denis, S., Mosser, D.D., Massie, B., 2002. The R1 subunit of herpes simplex virus ribonucleotide reductase protects cells against apoptosis at, or upstream of, caspase-8 activation. J. Gen. Virol. 83 (Pt. 11), 2779–2789.

Mastino, A., Sciortino, M.T., Medici, M.A., Perri, D., Ammendolia, M.G., Grelli, S., Amici, C., Pernice, A., Guglielmino, S., 1997. Herpes simplex virus 2 causes apoptotic infection in monocytoid cells. Cell Death Differ. 4 (7), 629–638.

Medici, M.A., Sciortino, M.T., Perri, D., Amici, C., Avitabile, E., Ciotti, M., Balestrieri, E., De Smaele, E., Franzoso, G., Mastino, A., 2003. Protection by herpes simplex virus glycoprotein D against Fas-mediated apoptosis: role of nuclear factor kappaB. J. Biol. Chem. 278 (38), 36059–36067.

Morse, L.S., Pereira, L., Roizman, B., Schaffer, P.A., 1978. Anatomy of herpes simplex virus (HSV) DNA: X. Mapping of viral genes by analysis of polypeptides and functions specified by HSV-1 × HSV-2 recombinants. J. Virol. 26 (2), 389–410.

Moy, R., Blaho, J.A., unpublished results.

Nguyen, M.L., Kraft, R.M., Blaho, J.A., 2005. African green monkey kidney Vero cells require de novo protein synthesis for efficient herpes simplex virus 1-dependent apoptosis. Virology 336 (2), 274–290.

Ozaki, N., Sugiura, Y., Yamamoto, M., Yokoya, S., Wanaka, A., Nishiyama, Y., 1997. Apoptosis induced in the spinal cord and dorsal root ganglion by infection of herpes simplex virus type 2 in the mouse. Neurosci. Lett. 228 (2), 99–102.

Patel, A., Hanson, J., McLean, T.I., Olgiate, J., Hilton, M., Miller, W.E., Bachenheimer, S.L., 1998. Herpes simplex type 1 induction of persistent NF-kappa B nuclear translocation increases the efficiency of virus replication. Virology 247 (2), 212–222.

Pereira, L., Wolff, M.H., Fenwick, M., Roizman, B., 1977. Regulation of herpesvirus macromolecular synthesis: V. Properties of alpha polypeptides made in HSV-1 and HSV-2 infected cells. Virology 77 (2), 733–749.

Perkins, D., Pereira, E.F., Aurelian, L., 2003. The herpes simplex virus type 2 R1 protein kinase (ICP10 PK) functions as a dominant regulator of apoptosis in hippocampal neurons involving activation of the ERK survival pathway and upregulation of the antiapoptotic protein Bag-1. J. Virol. 77 (2), 1292–1305.

Pomeranz, L.E., Blaho, J.A., 1999. Modified VP22 localizes to the cell nucleus during synchronized herpes simplex virus type 1 infection. J. Virol. 73 (8), 6769–6781.

Sanfilippo, C.M., Blaho, J.A., 2003. The facts of death. Int. Rev. Immunol. 22 (5–6), 327–340.

Sanfilippo, C.M., Chirimuuta, F.N., Blaho, J.A., 2004. Herpes simplex virus type 1 immediate-early gene expression is required for the induction of apoptosis in human epithelial HEp-2 cells. J. Virol. 78 (1), 224–239.

Sieg, S., Yildirim, Z., Smith, D., Kayagaki, N., Yagita, H., Huang, Y., Kaplan, D., 1996. Herpes simplex virus type 2 inhibition of Fas ligand expression. J. Virol. 70 (12), 8747–8751.

Taddeo, B., Esclatine, A., Roizman, B., 2002. The patterns of accumulation of cellular RNAs in cells infected with a wild-type and a mutant herpes simplex virus 1 lacking the virion host shutoff gene. Proc. Natl. Acad. Sci. U.S.A. 99 (26), 17031–17036.

Wallach, D., Varfolomeev, E.E., Malinin, N.L., Goltsev, Y.V., Kovalenko, A.V., Boldin, M.P., 1999. Tumor necrosis factor receptor and Fas signaling mechanisms. Annu. Rev. Immunol. 17, 331–367.

Yedowitz, J.C., Kotsakis, A., Schlegel, E.F., Blaho, J.A., 2005. Nuclear localizations of the herpes simplex virus type 1 tegument proteins VP13/14, vhs, and VP16 precede VP22-dependent microtubule reorganization and VP22 nuclear import. J. Virol. 79 (8), 4730–4743.